ELSEVIER

Ceramics International 30 (2004) 273–277

CERAMICS INTERNATIONAL

www.elsevier.com/locate/ceramint

Effects of Ni on the electrical conductivity and microstructure of $La_{0.82}Sr_{0.16}MnO_3$

Sutin Kuharuangrong

School of Ceramic Engineering, Suranaree University of Technology, Nakhon Ratchasima 30000, Thailand

Received 17 January 2003; received in revised form 24 March 2003; accepted 28 April 2003

Abstract

The effects of Ni doped into $La_{0.82}Sr_{0.16}MnO_3$ (LSM) have been studied. $La_{0.82}Sr_{0.16}Mn_{1-x}Ni_xO_3$ compositions with Ni content up to $x=0.3$ have been prepared by the solid state reaction and characterized to investigate the microstructure, thermal expansion coefficient (TEC) and electrical conductivity. A second phase detected by X-ray diffractometry has been found in all compositions after sintering at 1470 °C for 2 h. The results from scanning electron microscope show that the grain sizes of LSM reduce with Ni content and its TEC is changed insignificantly by Ni. The TEC value of 11.7×10^{-6} K^{-1} between 100 and 900 °C is obtained for $0\leqslant x\leqslant0.3$. The electrical conductivity from dc four point measurement indicates a trend of decreasing conductivity with increasing Ni content.

Keywords: C. Electrical conductivity; D. Perovskites

1. Introduction

Lanthanum strontium manganite (LSM) has been extensively studied as cathode for solid oxide fuel cell (SOFC). An increasing amount of Sr enhances the electrical conductivity of $LaMnO_3$ due to the increasing concentration of Mn^{4+}. However, Sr raises the thermal expansion coefficient (TEC) of $LaMnO_3$ resulting in mismatch with those of other components of SOFC. The composition of $LaMnO_3$ with 15–20 mol% strontium [1–4] is commonly used to investigate its properties. In addition, other divalent cations such as Ca, Mg and Ba are used to dope into A-site of this perovskite oxide, ABO_3. However, only Cr, Co and Ni have been usually selected for substitution on the B-site of LSM [5,6]. Co and Ni decrease the electrical conductivity of $La_{0.5}Sr_{0.5}MnO_3$ [5]. In contrast, Liu et al. [6] have reported that the addition of 0.1 mole fraction of Ni into Mn-site increases the electrical conductivity of $La_{0.6}Sr_{0.4}MnO_3$ but decreases that of $La_{0.82}Sr_{0.2}MnO_3$. This paper attempts to investigate the effect of Ni on the electrical conductivity of $La_{0.82}$ $Sr_{0.16}MnO_3$ including the microstructure and the thermal expansion coefficient. $La_{0.82}Sr_{0.16}MnO_3$ is selected to be lanthanum-deficient based composition for this work to enhance the chemical stability for the reactivity reduction of LSM toward YSZ electrolyte. The addition of 10, 20 and 30-mole% Ni as a dopant in this composition has been examined and properties compared with undoped material.

2. Experimental procedure

All compositions of undoped and Ni-doped $La_{0.82}Sr_{0.16}MnO_3$ were synthesized from La_2O_3, $SrCO_3$, Mn_2O_3 and NiO by solid state reaction route. 10, 20 and 30- mole% Ni were added and expected to substitute in Mn-site due to the similar ionic size. The total amount of cations on the B-site of perovskite oxide ABO_3 was one. The following abbreviation was used to identify each composition:

LSM for $La_{0.82}Sr_{0.16}MnO_3$,
LSMN1 for $La_{0.82}Sr_{0.16}Mn_{0.8}Ni_{0.1}O_3$,
LSMN2 for $La_{0.82}Sr_{0.16}Mn_{0.8}Ni_{0.2}O_3$ and
LSMN3 for $La_{0.82}Sr_{0.16}Mn_{0.7}Ni_{0.3}O_3$

E-mail address: sutin@ccs.sut.ac.th (S. Kuharuangrong).

0272-8842/03/$30.00
doi:10.1016/S0272-8842(03)00099-3

Before weighing, La_2O_3 raw material was calcined at 1000 °C to decompose either hydroxide or carbonate of lanthanum and the others were used as received. The non-stoichiometric compositions were prepared by milling with absolute ethanol in a polypropylene bottle. After drying, the mixture was calcined in air and the maximum firing temperature including the soaking temperatures during calcination were determined by differential thermal analysis (DTA, Perkin-Elmer DTA7). The phase of calcined powder was analyzed by X-ray diffraction (XRD, Jeol JDX3530). In addition, the lattice parameter was determined after correction of peak shift error in d-spacing with an addition of silicon as an internal standard. Disk or bar-shaped specimens were obtained after grinding and pressing the calcined powder. All compositions were sintered in air at 1470 °C for 2 h. The phase of fired samples was characterized by XRD to investigate any phase change after sintering.

The effect of Ni on the thermal expansion coefficient (TEC) of LSM was investigated by dilatometer (Netzsch, DIL402C). The data were collected from room temperature to 1000 °C with a heating rate of 3 °C/min.

The electrical conductivity of sintered bars using a dc four point method was measured as a function of temperature. Fired-on gold electrode was applied on the specimens before measurement. The data were collected from 100 to 900 °C with an increasing temperature of 3 °C/min.

The microstructure of sintered compositions was observed by scanning electron microscope (SEM, Jeol JSM5410LV). The samples were polished and thermally etched before examination.

3. Results and discussion

The results of differential thermal analysis for the mixed raw materials of LSM and LSMN3 compositions are represented in Fig. 1. The data show that the first two reactions occur in the range of 300–420 °C and 520–570 °C for both of LSM and LSMN3. However, the last reaction appears in different temperature ranges, 950–975 °C for LSM but 820–870 °C for LSMN3. Although the reactions from these results were complete before 1000 °C, the mixed powder of each composition in this work was calcined at the maximum temperature of 1200 °C and held at the temperatures which the reaction peaks occurred to obtain a uniform single phase. Fig. 2 shows the X-ray powder patterns of $La_{0.82}Sr_{0.16}Mn_{1-x}Ni_xO_3$ for $0 \leqslant x \leqslant 0.3$ after calcining at 1200 °C. The results indicate these compositions exhibit the characteristic pattern of a distorted orthorhombic crystal structure since the angle is close to 90°. There is no evidence of a second phase in the patterns. The calculated lattice parameters of all compositions after correction of peak shift are also listed in Table 1. The results show that with an increasing amount of Ni substituted into Mn, the lattice parameters of LSM decrease.

Fig. 3 shows the XRD patterns of undoped and doped LSM after sintering at 1470 °C for 2 h. The results exhibit the same phase present as revealed in Fig. 2. However, the appearance of a small peak at

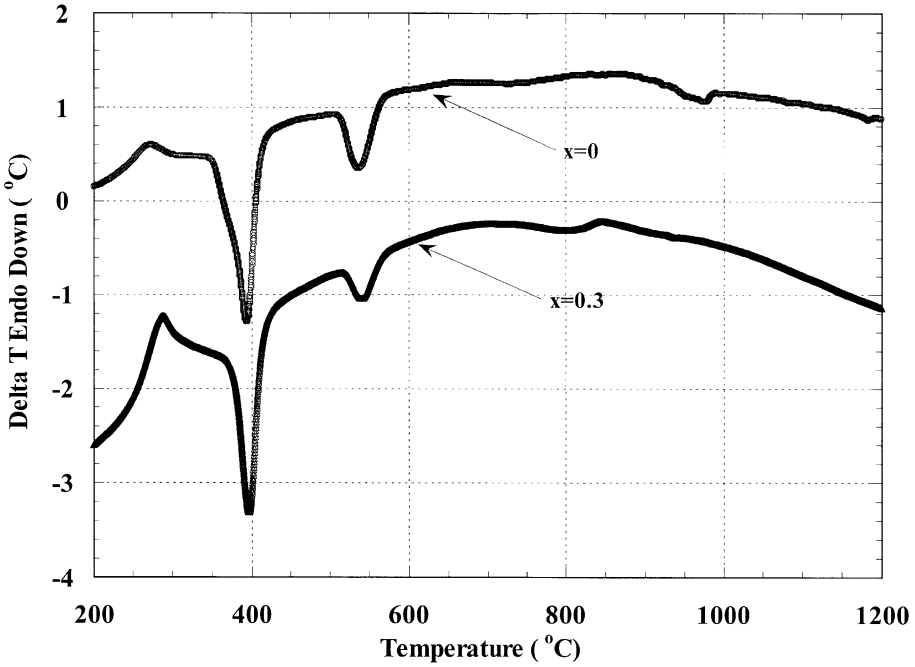

Fig. 1. DTA traces of the mixed raw materials for $La_{0.82}Sr_{0.16}Mn_{1-x}Ni_xO_3$.

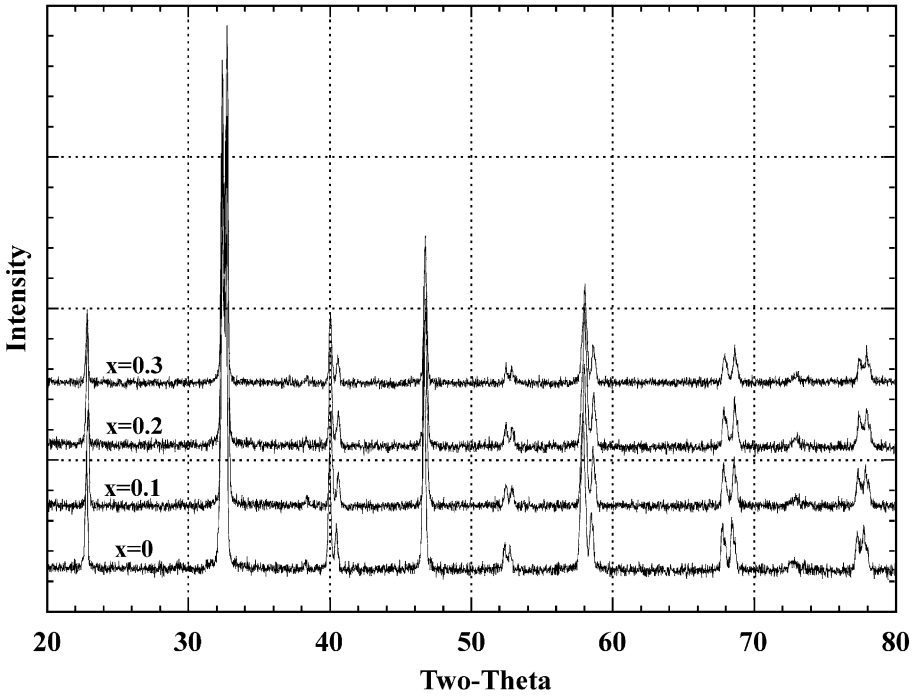

Fig. 2. XRD patterns of $La_{0.82}Sr_{0.16}Mn_{1-x}Ni_xO_3$ powder after calcining at 1200 °C.

Table 1
Calculated lattice parameter of LSM as a function of Ni concentration

Compositions	Lattice parameter (Å)		
	a	*b*	*c*
LSM	5.478	5.529	7.772
LSMN1	5.476	5.526	7.771
LSMN2	5.467	5.522	7.770
LSMN3	5.460	5.503	7.768

Table 2
Thermal expansion coefficient (TEC), the electrical conductivity at 900 °C and the activation energy as a function of Ni concentration

Composition	$TEC_{100-900\ °C}$ ($\times10^{-6}$ K^{-1})	Conductivity	
		$\sigma_{900\ °C}$ (S/cm)	E_a (kJ/mol)
LSM	11.7	107	12.9
LSMN1	11.5	92	16.1
LSMN2	11.7	68	15.8
LSMN3	11.8	48	18.0

$2\theta \approx 44.5°$ as pointed by the arrow could be observed in all sintered compositions. This suggests a second phase being possibly present after sintering at high temperature.

The effect of Ni-doped LSM on the thermal expansion coefficient (TEC) can be observed in Table 2. The experimental data measured from 100 to 900 °C indicate that the concentration of Ni does not have an influence on the expansion of LSM. The average TEC value of LSM and Ni-doped LSM is around 11.7×10^{-6} K^{-1}.

Fig. 4 illustrates the electrical conductivity of sintered compositions as a function of temperature. The data show that LSM has higher electrical conductivity than Ni-doped LSM through all measured temperatures. This is in agreement with the work of Carter et al. [5], in which $La_{0.5}Sr_{0.5}(Mn_{0.8}Co_{0.2})_{0.6}Ni_{0.4}O_3$ was reported to exhibit the lower electrical conductivity than the one without Ni. Nevertheless, the conductivity of the compositions with the lower amount of Ni was not given in the literature. From the result of Fig. 4 the conductivity of undoped LSM at 900 °C is 107 S/cm. With an addition of Ni into LSM, its conductivity decreases and further decreases with an increasing concentration of Ni. The electrical conductivity of Lanthanum manganite generally depends upon the amount of cation dopant with a lower valency and the available sites of Mn^{3+} changed to Mn^{4+}. Therefore, the maximum conductivity with divalent cation dopants on La-site (e.g. Sr, Ca) should occur around 50 mol% dopants since the available sites of Mn^{3+} and Mn^{4+} are equal. In this work, the available sites of Mn^{3+} are reduced attributing to the amount of Ni addition into $La_{0.82}Sr_{0.16}Mn_{1-x}Ni_xO_3$. Furthermore, the lattice parameter calculated from XRD results listed in Table 1 tends to decrease as the amount of Ni dopant increases. The ionic size of Ni^{2+} is larger than that of Mn^{3+} and Mn^{4+} [7]. These suggest that the oxygen vacancies possibly occur in Ni doped $La_{0.82}Sr_{0.16}Mn_{1-x}Ni_xO_{3-\delta}$. The electrons excited from oxygen vacancies may associate with holes hopping from Mn^{4+} to Mn^{3+}, resulting in the decrease of charge carriers. Consequently, the electrical

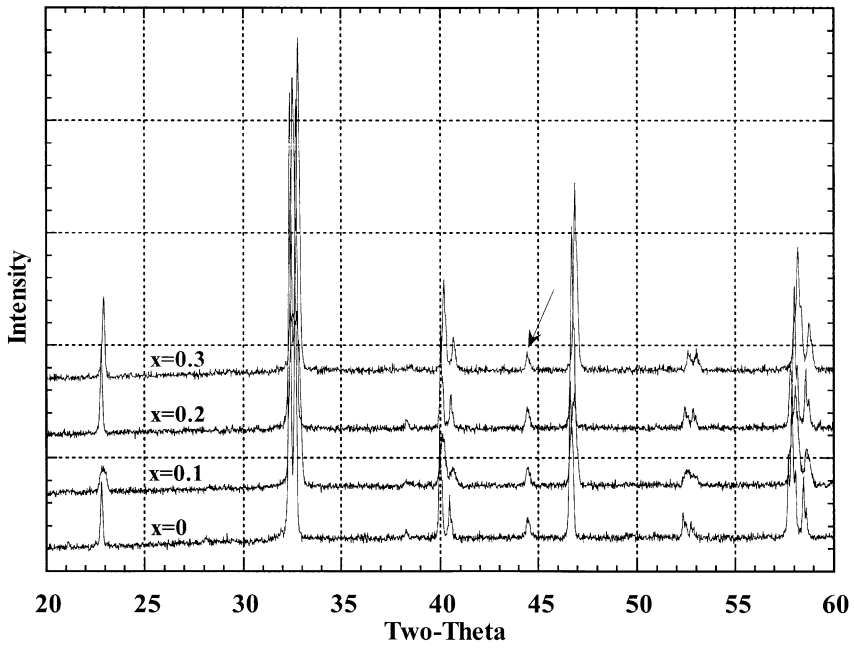

Fig. 3. XRD patterns of $La_{0.82}Sr_{0.16}Mn_{1-x}Ni_xO_3$ specimens after sintering at 1470 °C for 2 h.

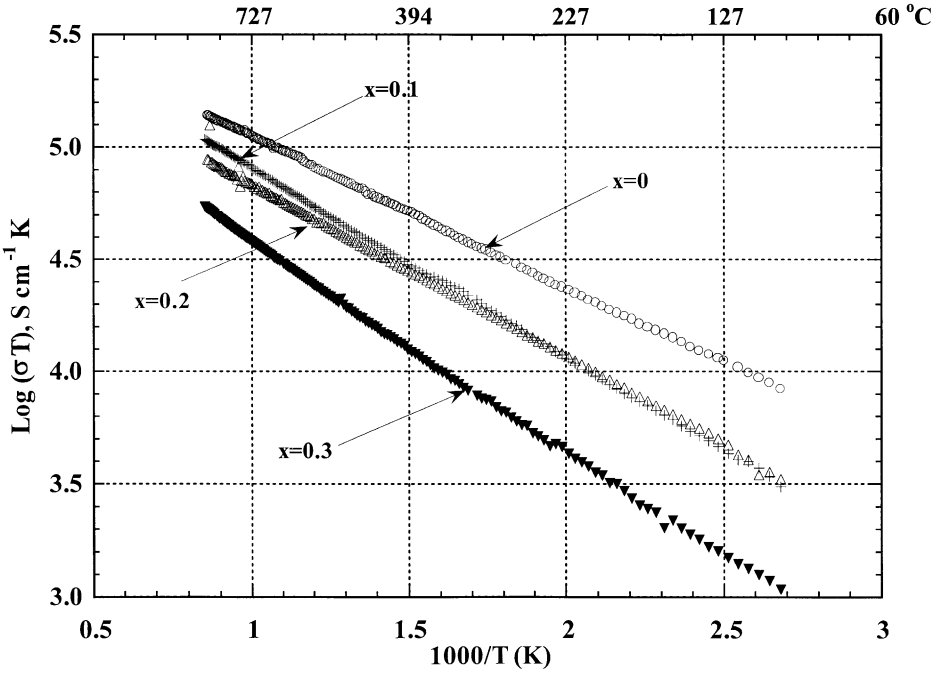

Fig. 4. Arrhenius plots of electrical conductivity of $La_{0.82}Sr_{0.16}Mn_{1-x}Ni_xO_3$.

conductivity of Ni-doped LSM reduces with the amount of Ni. The conductivity at 900 °C and the activation energy of each composition are also given in Table 2. The activation energy obtained from the slope of the data in Fig. 4 tends to increase with the concentration of Ni.

SEM photomicrograph of sintered LSM is shown in Fig. 5a. The average grain size is larger than 15 μm and both intergranular and intragranular pores could be observed in this composition. With Ni dopant, the grain size of LSM decreases with the increasing amount of Ni, resulting in a reduction of the intragranular pores as illustrated in Fig. 5b–d. It should be noted that the magnifications used for LSMN2 and LSMN3 are different from the others. Evidently, the grain size of Ni-doped LSM decreases, thus reducing the surface

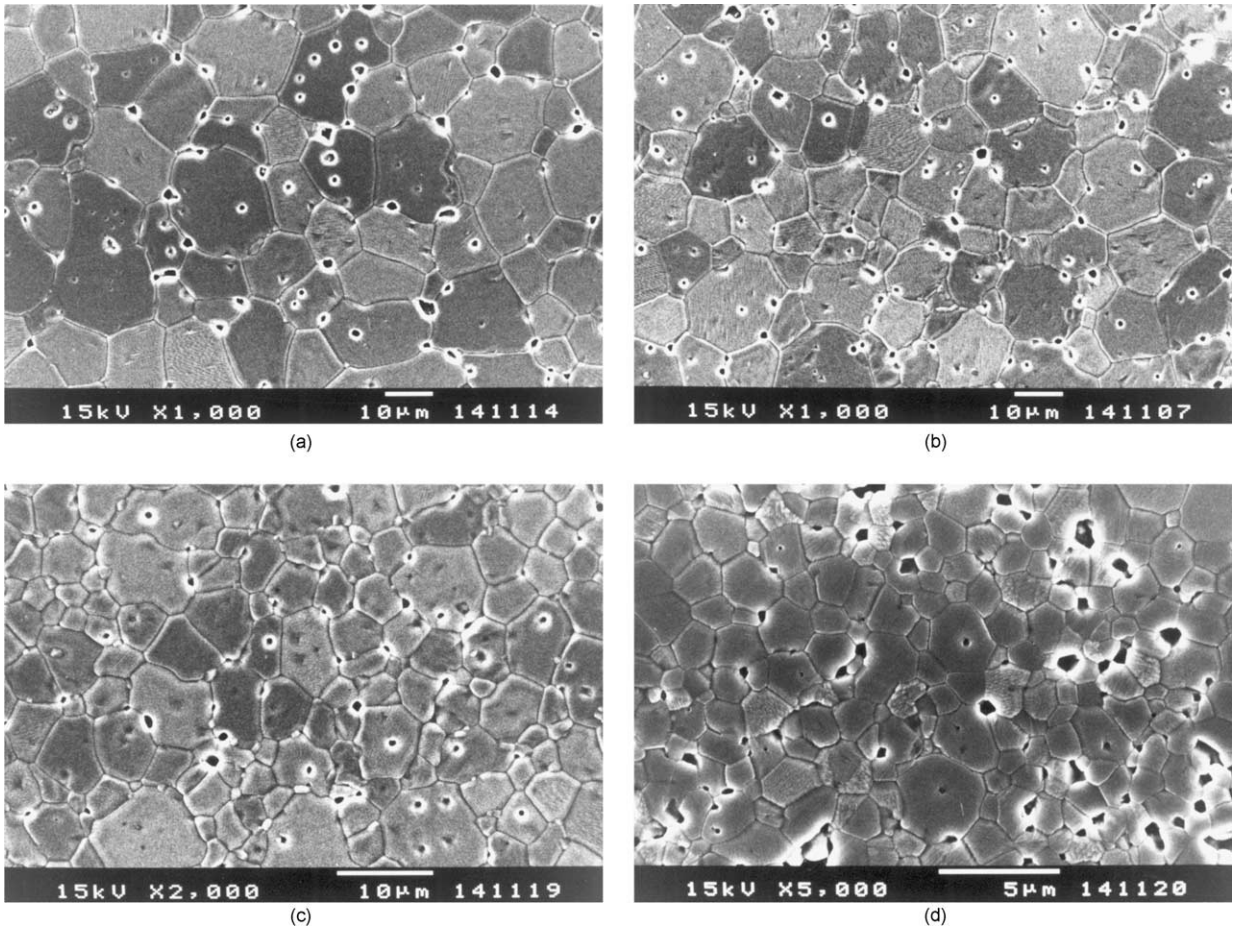

Fig. 5. SEM photomicrographs of compositions sintered at 1470 °C: (a) LSM, (b) LSMN1, (c) LSMN2, (d). LSMN3.

area. This effect is possibly related to the data of electrical conductivity, in which smaller grain size may also affect the lower conductivity.

4. Conclusions

Substitution of Ni into Mn insignificantly changes the TEC but reduces the electrical conductivity of LSM. As the amount of Ni dopant increases, the conductivity of LSM decreases and its activation energy also tends to increase. Furthermore, Ni inhibits the grain growth of this composition resulting in the decrease of surface area.

Acknowledgements

Financial support from Thailand Research Fund under the contract no. RSA/09/2544 is gratefully acknowledged.

References

[1] C.P. Jacobson, S.J. Visco, L.C. De Jonghe, Thin-film solid oxide fuel cells for intermediate temperature (500-800 °C) operation, Ceram. Trans. 109 (2000) 69–75.
[2] B.C.H. Steele, Survey of materials selection for ceramic fuel cells, II. Cathodes and anodes, Solid State Ionics 86–88 (1996) 1223–1234.
[3] M. Godickemeier, K. Sasaki, L.J. Gauckler, Electrochemical characteristics of cathodes in solid oxide fuel cells based on ceria electrolytes, J. Electrochem. Soc. 144 (1997) 1635–1646.
[4] T. Tsai, S.A. Barnett, Effect of LSM-YSZ cathode on thin-electrolyte solid oxide fuel cell performance, Solid State Ionics 93 (1997) 207–217.
[5] S. Carter, A. Selcuk, R.J. Chater, J. Kajda, J.A. Kilner, B.C.H. Steele, Oxygen transport in selected nonstoichiometric perovskite-structure oxides, Solid State Ionics 53–56 (1992) 597–605.
[6] X. Liu, W.-H. Shih, C. Wang, W. Worrell, Synthesis and characterization of $(La_{1-x}Sr_x)(MnNi_y)O_2$ perovskite as cathode for solid oxide fuel cell, Ceram. Trans. 109 (2000) 185–194.
[7] L.L. Hench, J.K. West, Principles of Electronic Ceramics, John Wiley & Sons, New York, 1990.